

# The Role of Tau in Network Dysfunction and Alzheimer's Disease Pathogenesis

By  
Allison Dombroski

Senior Honors Thesis  
Biology Department  
University of North Carolina at Chapel Hill  
19 March, 2019

Approved: 10 April, 2019

  
\_\_\_\_\_

Dr. Rick B. Meeker, Thesis Advisor  
Dr. Mohanish Deshmukh, Reader  
Dr. Graham Diering, Reader  
Dr. Elaine Yeh, Biology Faculty Sponsor

## **Abstract:**

Inflammation occurs early in the disease process of the Alzheimer's Disease (AD) mouse model and is believed to accelerate disease progression. When in the presence of AD pathological markers, inflammatory cells such as microglia release factors which lead to a disruption of homeostasis, including destabilization of intracellular calcium levels and cytoskeletal changes including modifications of the microtubule associated protein Tau. These changes are thought to increase the sensitivity of neurons to excitatory stimuli, leading to hyperactivity. However, the impact of this hyperactivity on neural communication within networks and the role of Tau are not well understood. To further understand the hyperactivity and neural dysfunction caused by these inflammatory factors, we used medium from microglia treated with A $\beta$  oligomers (A $\beta$ -MgCM) on cultured primary mouse neurons to mimic *in vivo* inflammation and compared the resulting electrophysiological recordings to the calcium changes in response to these challenges. Basal and inflammatory electrophysiological/calcium data were collected from microelectrode arrays (MEAs) for wild type (WT) and P301S/PS19 Tau-transgenic primary neural cultures to compare the effects of a pathological form of Tau on neural network function. Under basal conditions, the PS19 neurons showed increased calcium spikes which were often highly synchronized relative to WT neurons. Neurons expressing mutant Tau typically had a higher rate of action potentials within bursts, but exhibited shorter durations of bursts, as well as a lower node degree and higher path length, indicating poor functional connectivity within networks. Under inflammatory conditions induced by A $\beta$ -MgCM, both the WT and Tau transgenic (Tg) cultures displayed network disruption in response to the inflammatory stimulus. The finding that baseline P301S/PS19 neurons show aberrant development of neural network activity under both basal and inflammatory conditions that mimic

the very early stages of AD suggests that pre-tangle forms of Tau mediate neural dysfunction that may contribute to cognitive decline. This early dysfunction may provide opportunities for the development of new therapeutic strategies that slow the progression of AD.

## **1.0 Introduction:**

Alzheimer's disease (AD) is a fatal neurodegenerative disorder characterized by gradual cognitive decline and memory loss.<sup>1</sup> The only existent pharmacotherapies for AD provide minimal symptomatic relief and there are no current treatments to reverse or halt disease progression. This difficulty in treatment stems from the inability to diagnose Alzheimer's early due to the lack of known biomarkers early in disease progression. As more research is done on this disease, it is becoming increasingly evident that pathology arises long before any clinical manifestations.<sup>2</sup> There are two well-known primary late-stage pathological hallmarks of AD: amyloid- $\beta$  (A $\beta$ ) plaques, which are extracellular insoluble deposits derived from  $\beta$ -amyloid precursor protein (APP), and Neurofibrillary Tangles (NFTs), which are aggregates composed of hyperphosphorylated isoforms of the microtubule-associated protein tau.<sup>3</sup> Most AD research done in the past few decades has followed the amyloid cascade hypothesis, which states that A $\beta$  accumulation and deposition in the brain serve as the initiating events in AD progression. However, more recent findings have suggested that the original amyloid cascade hypothesis might require modification to incorporate a more central role for both Tau pathology and neuroinflammation in the pathogenesis of AD.<sup>1,4,5</sup>

Neuroinflammation, which is the activation of microglial cells by inflammatory stimuli, results in a cascade of effects that alter the functions of the nervous system and contributes in various ways to most neurodegenerative diseases.<sup>1</sup> Altered microglial activity can both accelerate

disease progression and trigger degeneration well before the appearance of more robust neurodegenerative markers like plaques.<sup>6</sup> Activated microglia serve to prune synapses, signal elimination of neurons, and secrete factors that could have either destructive or protective effects. Meeker et. al<sup>7-9</sup> have previously shown that soluble factors released by activated macrophages and/or microglia cause an accumulation of neuronal calcium, cytoskeletal dysfunction, and increased N-methyl-D-aspartate (NMDA) receptor sensitivity on neurons, much like the changes seen in early AD pathology.<sup>10</sup> Focal swellings in the axons and dendrites follow the calcium influx and accumulate modified forms of tau.<sup>15</sup>

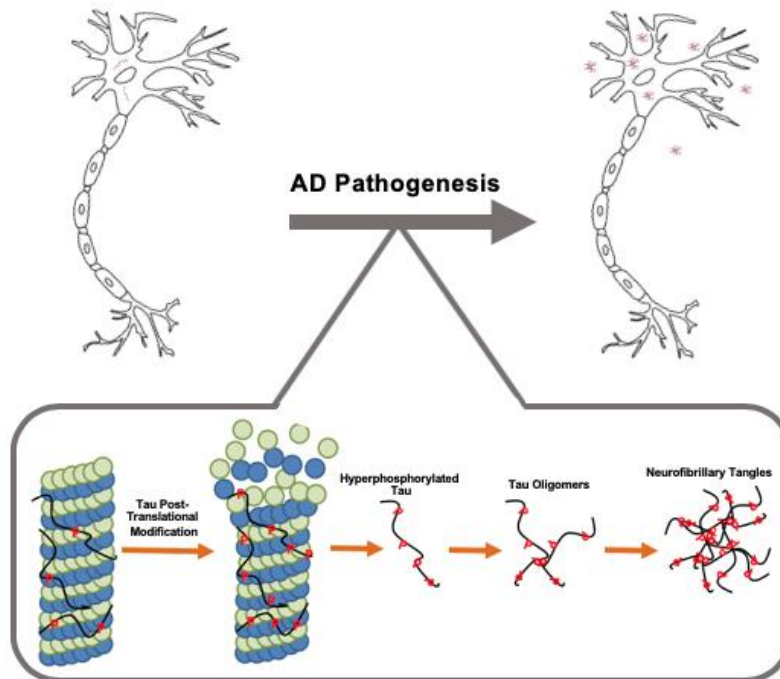


**Figure 1:** In Alzheimer's disease (AD) the microtubule stabilizing protein, Tau, is abnormally hyperphosphorylated and becomes prone to oligomerization. These Tau oligomers eventually aggregate into insoluble neurofibrillary tangles (NFTs), which are believed to contribute to neuronal death and facilitate further disease progression.<sup>1</sup> The Tau P301S/PS19 Tg mice in this project were genetically mutated to express the mutant form of Tau that is associated with the development of NFTs. This mutant form is more prone to form beta-pleated sheets/oligomers and mimics the gradual progression of *in vivo* Tauopathies.

To examine the functional impact of early Tau modifications we used the PS19 mouse model to track the evolution of Tau pathology shown in Figure 1. This model is genetically modified to express the human P301S mutation that is found in Frontotemporal Dementia and other tauopathies. The PS19 mouse model is useful in Alzheimer's Disease research because it expresses accelerated neuroinflammation and Tau pathologies that would otherwise take much longer time to develop, both *in vivo* and *in vitro*.<sup>11</sup> In previous experiments with the PS19 mice, inflammation and synapse loss preceded the formation of NFTs or plaques, and these neurons showed more hyperexcitability under both basal and inflammatory conditions.<sup>6</sup> Network dysfunction therefore may develop early in AD progression and contribute significantly to cognitive decline. Both early Tau pathogenesis and neuroinflammation may serve as excellent targets for therapeutic interventions to slow cognitive decline in AD patients.

To develop better therapies for neurodegenerative diseases such as Alzheimer's, there must be a better understanding of the early biological events that trigger the pathological cascade. In this study, we performed *in vitro* electrophysiological and calcium imaging analyses to investigate our hypothesized relationship between neuroinflammation, Tau, and subsequent dysregulation of neural networks. To test our expected role of Tau in disease progression, PS19 Tau Tg mouse neurons were analyzed and compared to wild-type (WT) neurons under various experimental conditions. Primary mouse neurons were cultured on a low-density, 60-electrode, microelectrode array (MEA) (MEA 1060BC, Multi Channel Systems, Inc., Reutlingen, Germany) to measure the activity of neural circuits over time. The analysis of network function included measures of population viability (% active electrodes; detects dropout of neurons), number of synchronous bursts, spike rates within bursts, burst length ("inhibitory" feedback), characteristics of burst recruitment (rate of development of bursts), connection weights (fidelity

of neuron-neuron communication), path length (efficiency of connections), node degree (extent of connectivity from “hubs” of activity), and degree centrality (relative efficiency of connections).<sup>12</sup> Changes in electrophysiological activity were measured along with the disruption of calcium homeostasis in these neurons using live cell imaging. In experimental conditions, the mouse neurons were challenged with inflammatory stimuli produced by cultures of mouse microglia that were exposed to A $\beta$  oligomers. The effects of the inflammatory challenge on neural network activity were then analyzed to determine how inflammatory factors produced in response to hallmark AD oligomers alter the activity of neurons. We found significant structural and electrophysiological dysfunction in the neural networks formed by PS19 neurons compared to the WT control, as well as differences in the effects of neuroinflammation on the dysregulation of PS19 and WT neurons.

## **2.0 Materials and Methods:**

### **2.1 Primary Neural Cell Cultures**

All animal work performed followed the NIH animal welfare guidelines and were approved by the UNC Institutional Animal Care and Use Committee (IACUC approval 16-129.0). Pregnant female Long Evans mice (Charles River) were euthanized at gestational day E16 using a lethal dose of isoflurane. After confirmation of death by clipping the heart, the mother’s uterus was excised and the fetuses were placed in HEPES-buffered Hank’s balanced salt solution (HBSS). Each fetus was individually genotyped and sorted (WT vs. Tau Tg). The fetal mice brains were then removed and rinsed three times in sterile HBSS. The forebrains (cortex and hippocampus) were isolated from each brain and incubated for 30 minutes at 37°C in Ca<sup>2+</sup>-Mg<sup>2+</sup>-free HBSS (CMF-HBSS) + 10 U/mL papain + 2.5 U/mL DNase I. The resulting

tissue was gently triturated to produce a single-cell suspension and diluted in Neurobasal Plus + B27 Plus + 5% Fetal Bovine Serum (FBS) + 0.5 mM glutamine + 20 µg/mL gentamicin. The dissociated neural cells were then seeded into poly-D-lysine-coated culture dishes containing coated coverslips at a density of 10,000-20,000 cells/cm<sup>2</sup> for later calcium imaging.

The MEA grid was coated with 0.005% Polyethylenimine (PEI) and laminin and dissociated neurons were seeded at a density of 50,000 cells/cm<sup>2</sup>. After attachment, the cultures were grown at 37°C with 5% CO<sub>2</sub> and fed three times per week with Neurobasal Plus + B27 plus + 10% FBS + 0.5 mM glutamine + 20 µg/mL gentamicin with 50% medium exchange. Cultures were almost purely neuronal and were used at 8-42 days in vitro (DIV) to track the development of pathology. Cell viability, extent of dendrite outgrowth, and the appearance of morphological features of damage such as beading was monitored in the MEA cultures.

## **2.2 Preparation of Microglia and Conditioned Media:**

Primary microglia grown from gestational E16 fetal mice brain micro-explants were cultured on ultra-low adhesion plastic to maturation in a neural environment to mimic *in vivo* conditions. The microglia grew within the explants and were fed three times per week with DMEM-H (Gibco) + 10% FBS (Gibco HI FBS, 10082-139)+ 20 µg/mL gentamicin. After approximately 3 weeks *in vitro*, a monolayer of highly purified microglia had migrated from mice brain explants to the surface of the plate. Any glial or neural cells still in suspension were removed and the purified population of microglia was challenged for 1 hour with an inflammatory stimulus (Aβ<sub>o</sub>) to recapitulate the pathological conditions associated with inflammation. The resulting medium was collected and centrifuged at 1000 x g to remove particulate material. The supernatant was then ultrafiltered at 300 kDa MWCO. Using calcium

imaging, we verified the toxicity of the ultrafiltrate at a dilution of 1:5 on primary mouse neurons grown on coverslips.

### **2.3 MEA Electrophysiology:**

The methodology for electrophysiological recordings followed the procedures outlined by Pan et al., (2015).<sup>13</sup> MEA's from Multichannel Systems (MCS, Reutlingen, Germany) consisted of 60 TiN<sub>3</sub> electrodes with diameters of 30 µm and spacing of 200 µm, one of which served as a ground. The spontaneous activity on the MEA's was measured using an MCS 1100x amplifier at 25 kHz sampling with a hardware filter of 300-3000 Hz at 37°C under continuous flow of sterile 5% CO<sub>2</sub> air. A Teflon membrane was used to reduce evaporation and chances of contamination, as outlined in Potter and DeMarse, 2001.<sup>14</sup> MCRack software was used to record up to 4-week old cultures for 5 minutes of spontaneous activity approximately every 3 days beginning on day 10. The action potential spikes were sorted and recorded only if they surpassed the negative threshold of 5 times the standard deviation estimated from the background noise. Our analysis of electrophysiological data was conducted using custom python (Enthought 64-bit v1 .2), C, C++ code. Electrodes were pooled among each group for statistical analysis and compared using two-tailed Student's t-tests for independent samples. P values of less than 0.05 were considered significant. All error values in text and figures represent +/- the standard error of the mean



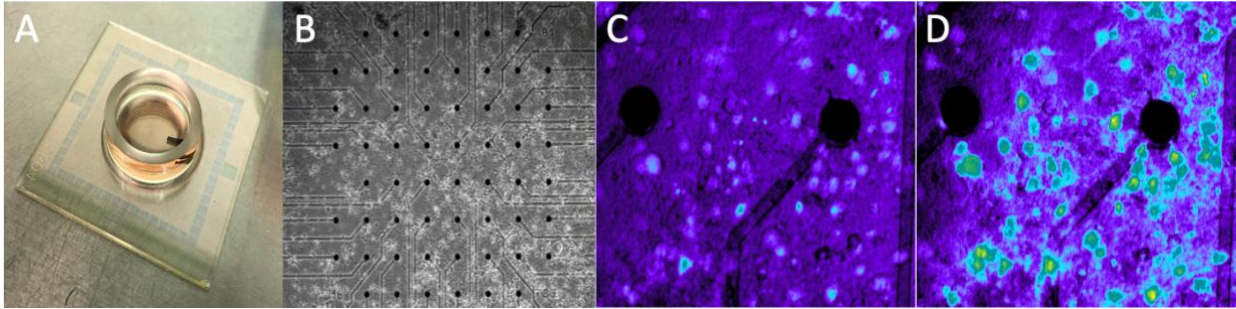


**Figure 2.** (A) An 8x8 extracellular microelectrode array records spontaneous activity of thousands of dissociated and cultured neurons harvested from either WT or Tau P301S mice. (B) Image taken at 4X magnification of full 60-electrode MEA containing cultured neurons. (C-D) Images taken before (C) and during (D) a calcium spike event by WT neurons cultured on an MEA under basal conditions

## 2.4 Intracellular Calcium Imaging:

Changes in intracellular calcium regulation were imaged in both the WT and Tau Tg neurons cultured on MEAs or coverslips. The neuronal cultures on coverslips were prepared for calcium imaging by washing them with artificial cerebrospinal fluid (aCSF: 127 mM NaCl, 5.0 mM KCl, 2.3 mM CaCl<sub>2</sub>, 1.3 mM MgCl<sub>2</sub>, 20 mM glucose). The rinsed cultures were incubated for 30 minutes at a 3:1 dilution in aCSF to fluorescent calcium indicator Fluo-4 AM (2  $\mu$ M, Molecular Probes Inc., Eugene, OR). Following incubation, the neuron-coated coverslips were mounted on a stage for imaging via fluorescence microscopy on an Olympus IMT-2 inverted microscope at 20X magnification. 320  $\mu$ L of aCSF were added to the coverslip to prevent drying of the cells. Cells were imaged every 6 seconds for 6 minutes during the acute phase with 40 ms fluorescent exposures using the quantification program Metamorph (Molecular Devices, Downingtown, PA). Once the acute phase began, the cultures were challenged with 80  $\mu$ L of an inflammatory stimulus (MgCM) or a control solution (aCSF), leaving a final dilution of 1:5. Following completion of the acute phase, delayed phase images were taken automatically every 60 seconds for 1 hour to assess the development of sustained calcium dysregulation. The

fluorescence levels were quantified in individual neurons using Metamorph and Microsoft Excel to assess calcium dysregulation.

Neurons cultured on MEAs were prepped and loaded with Fluo-4 AM similarly to those on coverslips except they were maintained in Neurobasal medium to prevent any perturbation of the electrical activity and to facilitate sequential temporal analyses. Intracellular calcium levels were monitored and recorded simultaneously with electrophysiological recordings of the MEAs, as outlined in Figure 3.

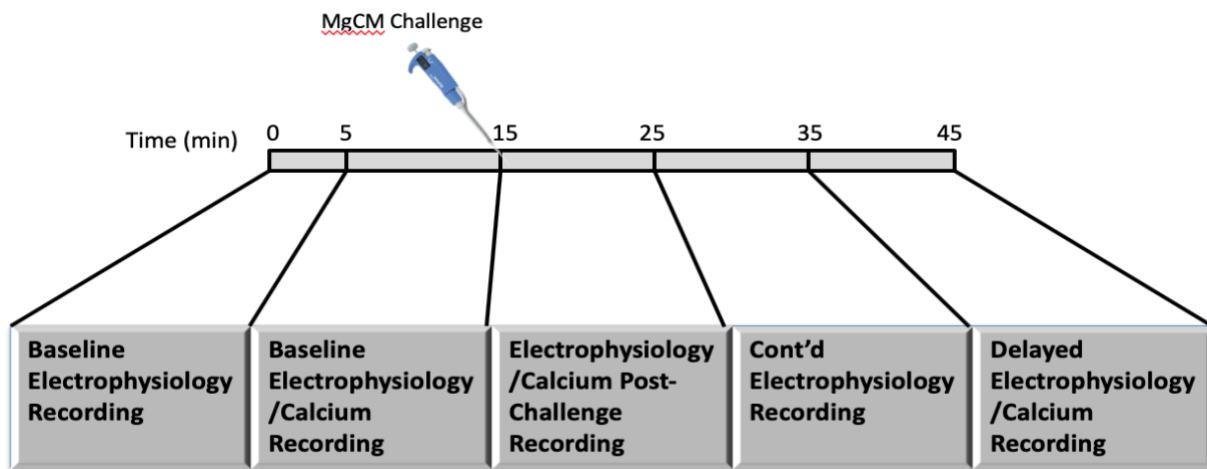


**Figure 3.** Timeline of recording of joint electrophysiology and calcium readings for a typical run of either WT or PS19 neurons in response to an inflammatory stimulus. Neurons on the MEA were stimulated with MgCM at a 1:5 dilution at  $t = 15$  minutes.

## **3.0 Results:**

### **3.1 Developmental Differences in Tau Tg Neurons**

To attempt to fill the gap in literature regarding the effects of pathological Tau on the brain during early disease development, we compared electrophysiological data between WT and PS19 neurons over time in culture. During this developmental stage (4-5 weeks *in vitro*), both

WT and PS19 neurons established highly connected, synchronous neural networks (WT example in Figure 4). These circuits developed bursting patterns in which localized neural activity spreads activation of neurons across the majority of electrodes on the MEA.

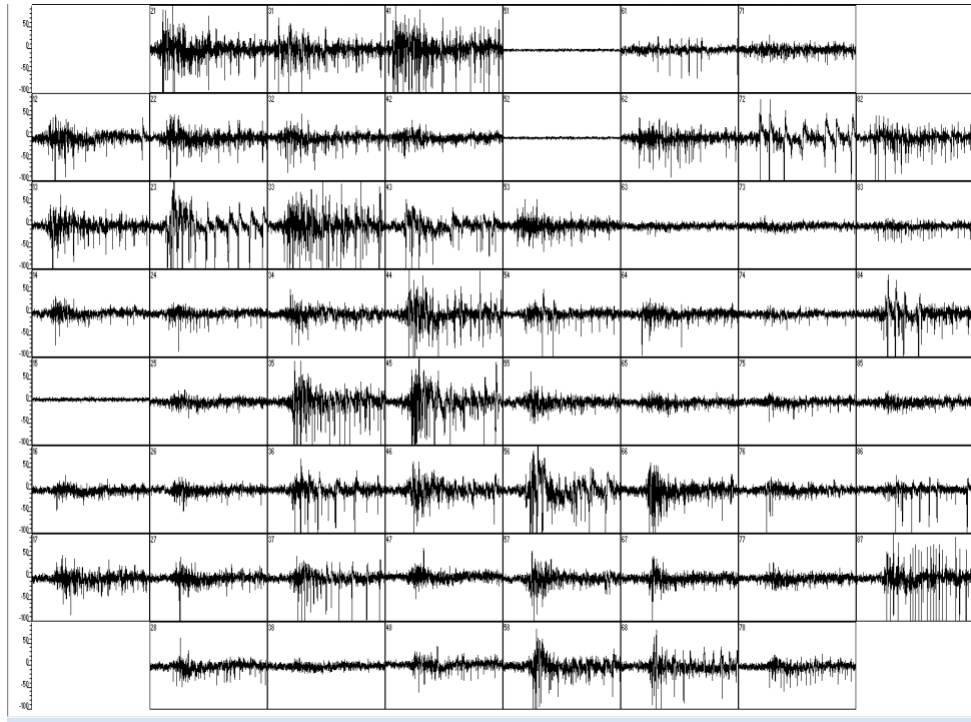


**Figure 4: Example of Spontaneous Neural Firing Recorded by MEAs.** Image was captured from an electrophysiological recording of WT neurons at 24 DIV under basal conditions. Individual boxes correspond to a separate electrode on the full MEA, and the spikes correspond to action potentials recorded from neurons localized near each electrode. Synchronous bursting patterns across the MEA indicate a highly interconnected circuit, which is characteristic of neural cultures at this age.

While both WT and Tau Tg neural cultures displayed synchronous network activity throughout development, our analyses showed fundamental differences in the behavior and physical properties of PS19 networks versus WT controls. As is shown in Figure 5 and Figure 6D, PS19 neurons exhibited shorter bursts than WT. PS19 neural cultures also had significantly less widespread activity and slower mean firing rates (MFRs) than WT controls until late stages

of network development (Figure 6A-B). Though these Tau Tg neurons had lower MFRs and shorter bursts, they did exhibit significantly higher rates of bursting (Figure 6C).

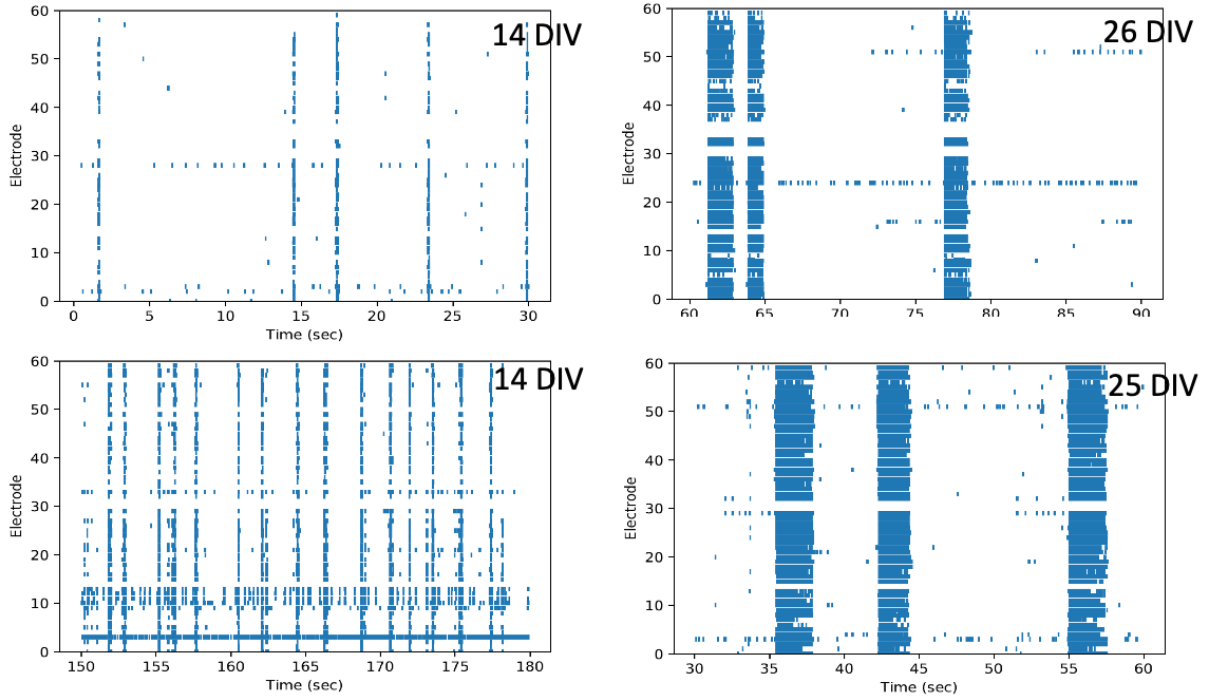


**Figure 5.** Raster plots created from developmental electrophysiological data illustrate the synchronization of bursting activity across the 60 electrodes over the course of development for PS19 neurons (top) and WT neurons (bottom). Blue lines represent the firing of neurons at a specific electrode (y-axis) at different times in the recording (x-axis). The thick vertical lines indicate synchronized neural bursts.

Tau pathologies including hyper or hypo excitability and potential synapse loss or decrease in synaptic function could have a profound effect on the structure of developing PS19 networks relative to their wild type controls. Any systematic synapse “loss” due to Tau over-expression might appear as a reduced number of functional connections among neurons in PS19 networks. The functional connectivity between electrodes was estimated from spike trains based on a scaled cross correlation. Figure 7A depicts the node degree (functional connections) of electrodes on MEAs and shows a significant reduction in connections expressed by PS19 networks during development up to day 20 in culture. During the last few weeks of development,

there was higher variability in the node degree of PS19 networks, with some connections having dramatically low or high degrees, though the average was still consistently lower than the average WT node degree. The lower node degree in PS19 networks was associated with significantly higher average path lengths across the networks (Figure 7B), suggesting overall reduced network efficiency during communication in these Tau Tg neurons.

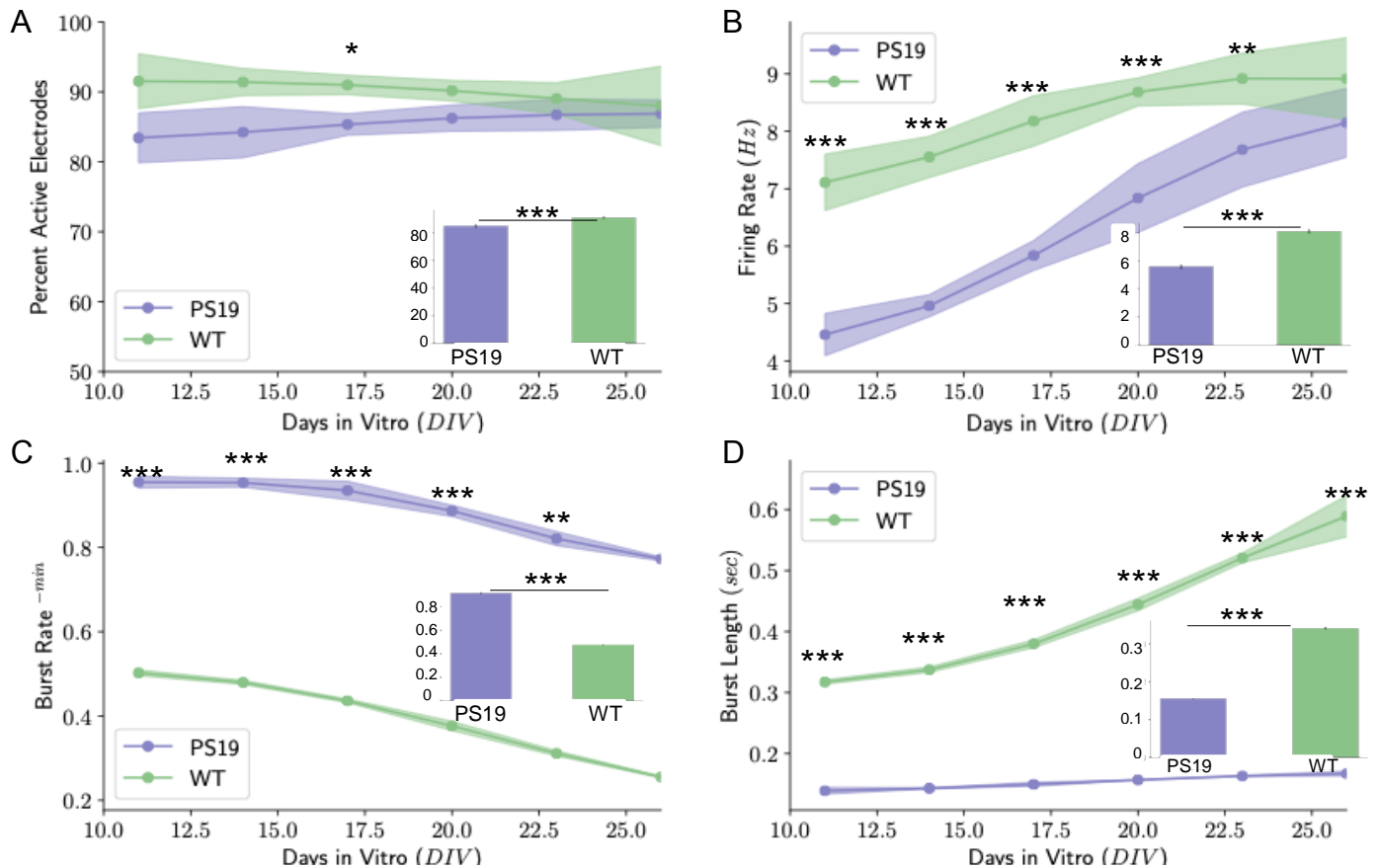


**Figure 6.** Our electrode arrays were able to detect differences among neurons in PS19 relative to wild type early in the development of these networks in culture. All cultures were plated at the same initial spatial density. However, **panel A** shows that the percentage of electrodes that contained active neurons with normal firing rates  $> 0.01$  Hz was lower in PS19 than WT. **(B)** Tau overexpression also resulted in neuron assemblies that fired significantly slower on average but had increased burst rates (**panel C**) with shorter burst durations than WT controls (**panel D**). Insets in each panel represent comparison of the average values across all points in development for WT and PS19 cultures. For PS19,  $n$  ranged from 4-13 depending on the day in vitro. For WT,  $n$  ranged from 3-10.  $** = p < 0.01$ .  $*** = p < 0.001$ .

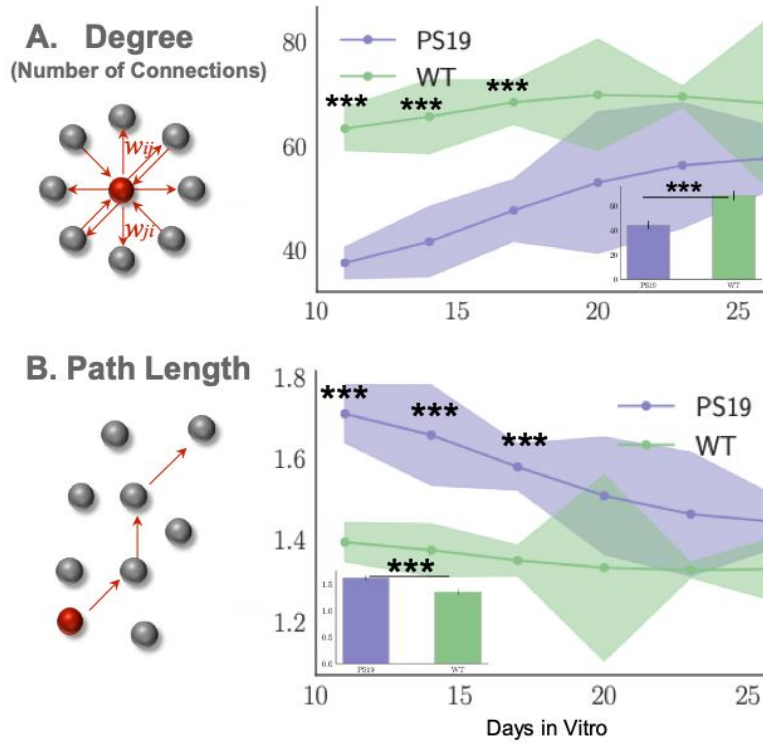


**Figure 7. (A)** The average number of functional connections (i.e., the node degree) per electrode. The reduced functional connections were associated with significantly higher average path lengths across the networks **(B)**. Insets in each panel represent comparison of the average values across all points in development for WT and PS19 cultures. For PS19, n ranged from 4-13 depending on the day in vitro. For WT, n ranged from 3-10. \*\*\* =  $p < 0.001$ .

### 3.2 Homeostatic Calcium Changes in WT/PS19 Neurons

As calcium is heavily involved in many signaling cascades within cells, we expected to see increases in intracellular calcium in accordance with increased electrophysiological activity. Our attempts to correlate precise increases in MFRs with calcium spikes showed a poor relationship (Figure 8B).

Though we were not able to show a direct relationship between calcium spiking and increased bursting, we still compared calcium homeostasis in the PS19/WT neurons on low-density coverslips to pinpoint any differences in the function of individual neurons. We found that at the same stage in development, PS19 neurons exhibited enhanced intrinsic calcium

spiking when compared to the WT control (Figure 9). This is consistent with a hyperexcitable state of neurons.

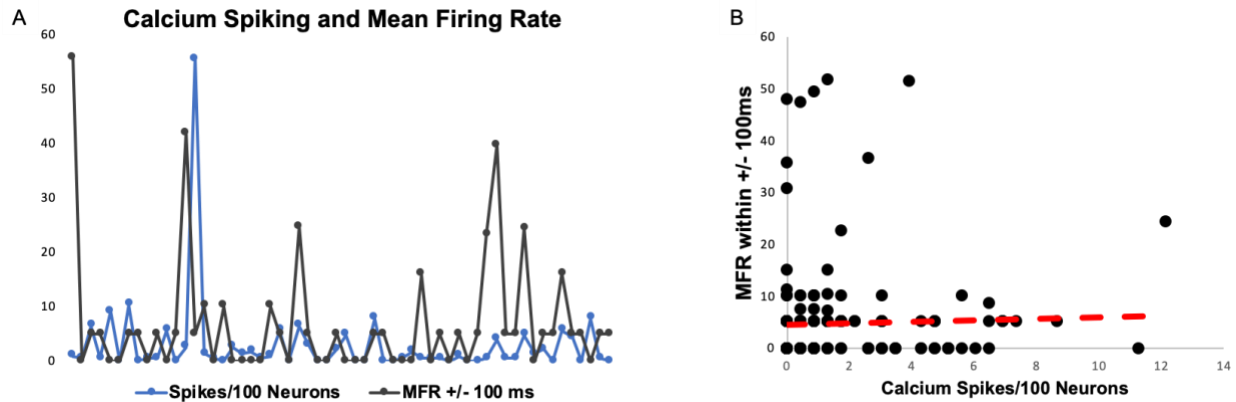


**Figure 8.** (A) Overlap of average calcium spikes per hundred neurons with increases in mean firing rates shows some concordance, but correlative analysis in (B) shows that though it was expected, there seems to be no clear direct linear relationship between calcium spiking and increased rates of neural bursting (red line).

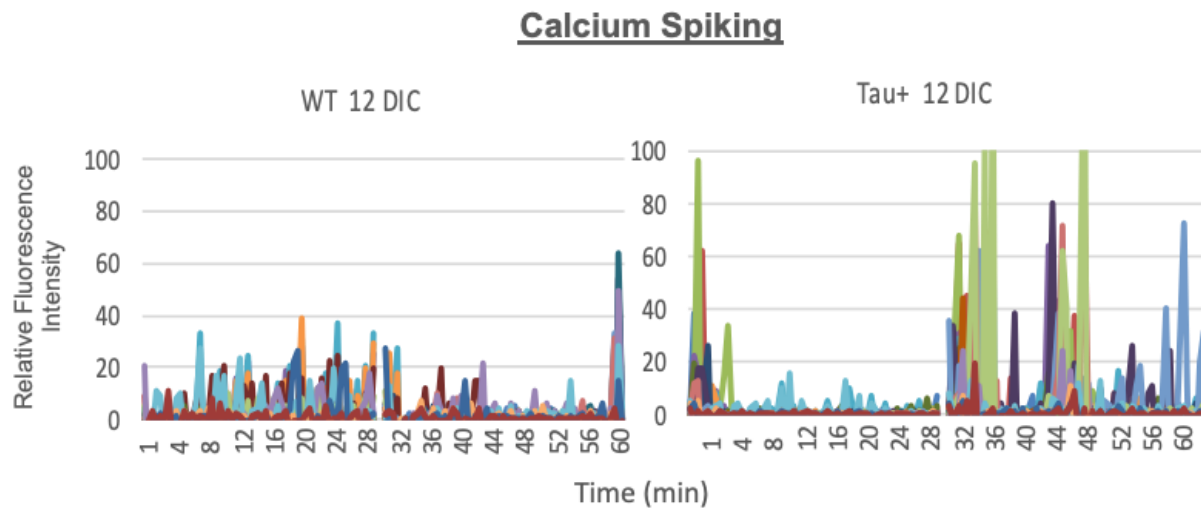


**Figure 9.** Intrinsic calcium spiking in WT and PS19 neurons at 12 days in culture under basal conditions. Each individual peak represents the relative fluorescence, and thus calcium levels, of one neuron.



### 3.3 Effects of Inflammation on PS19/WT Neurons

Neuroinflammation is known to be an important factor in advancing the pathology of neurodegenerative diseases such as Alzheimer's. When primary neurons are introduced to medium containing factors secreted from inflammatory cells, an acute spike in intracellular calcium is observed, followed by a delayed accumulation. In accordance with this calcium dysregulation is the buildup of beads along the dendrites, which test positive for modified Tau, as well as other pathological markers.<sup>15</sup> This neuroinflammation likely acts synergistically with the PS19 mutation to contribute to the pathological phenotype. We were therefore interested in how PS19 neurons would react under inflammatory conditions when compared to the WT control on coverslip cultures. We found that while PS19 calcium levels did increase in response to conditioned medium, the effect was much smaller compared to the WT increase in calcium (Figure 10).

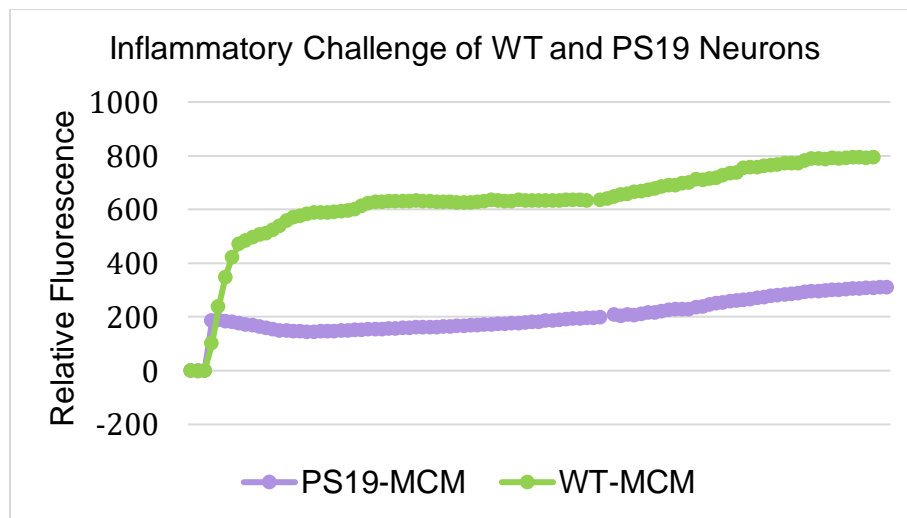


**Figure 10:** Relative calcium levels in PS19 and WT neurons cultured on coverslips over a 40-minute time course following inflammatory stimulation with macrophage conditioned medium (MCM). The delayed increase in intracellular calcium characteristic of inflammatory challenge is shown to be decreased in PS19 neurons.



Administration of A $\beta$ -MgCM to neurons cultured on the MEAs resulted in an acute rise in mean firing rate (MFR) that gradually dissipated for both neural populations. Interestingly, the inflammatory stimulus had less of a boosting effect on the MFR of PS19 neurons, though it is important to note that the baseline MFR was significantly lower in PS19 cultures to begin with (Figure 11A). Both WT and PS19 neurons also drastically increased their rate of bursting in response to the conditioned medium before returning to baseline, with a greater acute increase in the PS19 cultures. There was an opposite effect of the MgCM on the peak MFRs within neural bursts in the two neural populations (increase in WT, decrease in PS19, inset of Figure 11B).

In terms of physical properties of the networks in response to inflammation, we observed a significant decrease in WT node degree post-stimulation, which returned back to baseline, indicating an acute loss of network function. An opposite effect of an acute increase in PS19 node degree was seen, suggesting a transient enhancement of network function (Figure 11C). The lower loss of function in the PS19 neurons was consistent with the reduced calcium dysregulation. We also found a significant increase in WT path length following stimulation, indicative of a deleterious effect on network functioning from neuroinflammation. However, there appeared to be a less significant effect of the stimulus on PS19 path length (Figure 11D).

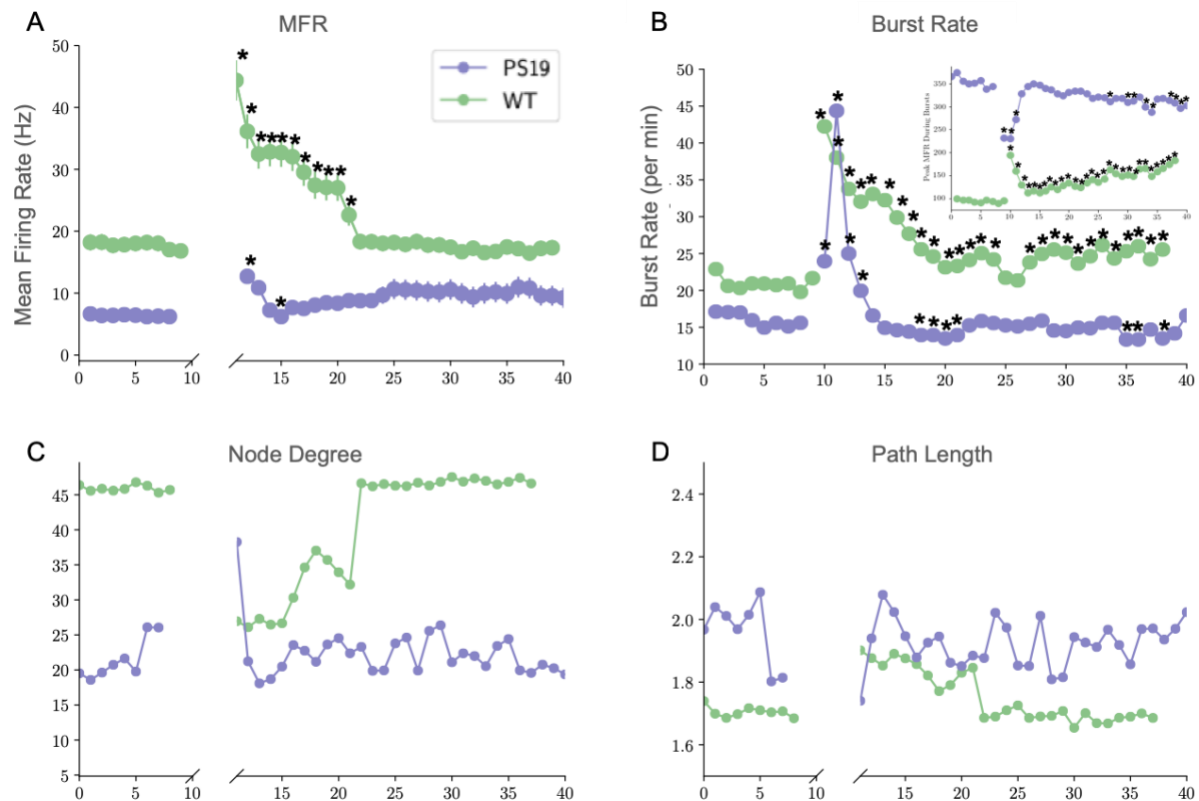


**Figure 11.** Network electrophysiology during a 10-minute baseline recording and 30 minutes following stimulation with A $\beta$  conditioned medium. **(A)** Mean Firing rate estimates were assembled from 2-minute activity windows every 60 seconds during the recording. **(B)** Effects on network bursting included a significant increase in burst rates during the first 20 min for both groups of cells. Inset shows PS19 neurons achieve higher peak MFRs within these bursts. **(C)** The number of functional connections (node degree) were significantly reduced at first for WT and then returned to baseline. There was an acute rise in functional connections in PS19 neurons post stimulation, but it soon returned to baseline as well. Path length shown in **(D)** significantly increased for WT, while there appears to be a lesser effect of the media on PS19 path length. For PS19,  $n = 4$ . For WT,  $n = 9$ .

## 4.0 Discussion:

We investigated whether or not the aberrant Tau in P301S/PS19 mouse neurons contributed to a pathological phenotype and if neuroinflammation accelerated this early pathology. We found that during the course of network development *in vitro*, PS19 neurons exhibited slower average firing rates than WT controls. Interestingly, these same PS19 neural

networks bursted at a higher rate, with shorter burst durations, than WT networks. These shorter burst lengths of PS19 neurons may be secondary to their propensity to burst at a higher rate. Any longer bursts at such a high rate, with a shorter refractory period in between, would restrict the ability to sustain the burst.<sup>16</sup> All together, these findings support the hypothesis that early modification of Tau on the cellular level can lead to a hyperactive phenotype, which is potentially obscured by the lower average firing rates at baseline. More data is required to solidify this hypothesized hyperexcitability in PS19 neurons and its proposed implications on neuronal function throughout network development.

Also consistent with our hyperexcitability hypothesis are the findings that PS19 neurons exhibited enhanced intrinsic calcium spiking under baseline conditions when compared to the WT control (Figure 9). Calcium spiking is positively correlated with cell signaling and enhanced activity, so these data support our claim that under the influence of no extraneous stimuli Tau Tg neurons show intrinsic differences in cellular signaling compared to WT neurons at baseline. However, our attempts to correlate increased intracellular calcium with bursting activity have not yet been successful (Figure 8). While this lack of a relationship was not expected, it indicates that remodeling our analysis may provide a clearer picture of how electrophysiology and calcium signaling are related. More research is required to discern the role of these calcium events in network decline, specifically the role of calcium in the misfolding of Tau and the subsequent disruption in intracellular transport and how this affects neuronal dysfunction.

With regard to the physical characteristics of the neural networks developed by the PS19 neurons, we found evidence for significant degradation amongst Tau networks compared to the WT. We observed an increase in average path length (number of times a neuron has to intermittently relay a message to get it from point A to point B) in the PS19 networks. We also

assessed the functional connectivity of these networks and found a significant decrease in node degree in Tau networks (Figure 7). This is all indicative of dysfunctional network development and reduced communication efficiency in PS19 networks relative to WT controls. This handicap of developing PS19 networks could be caused by the accumulation of deficits of a large number of neurons within the networks, or by dropout/death of a small population of cells such as GABAergic inhibitory cells within these networks.<sup>4,17</sup> Either possibility would be secondary to the development of early Tau pathology. This supports our hypothesis that early Tau pathology, in the absence of any plaques or tangles, could have a significant effect on neural network function and may contribute to early disease progression.

Our results indicate that inflammatory factors released by activated microglia have significant destabilizing effects on both WT and Tau Tg neurons in terms of electrophysiological activity and calcium homeostasis (Figure 10 and 11). Previous studies have shown that activated inflammatory cells have direct effects on intracellular calcium homeostasis.<sup>10</sup> Calcium dysregulation from neuroinflammation is shown not only via a gradual increase in intracellular levels of calcium (Figure 10), but it is also seen in the change in excitability of the neurons over time. Just as the conditioned media caused an upsurge in neural calcium levels, it also caused a rapid increase in the average firing rates of both populations of neurons in culture, which returned to baseline over time (Figure 11). We found that the inflammatory stimulus generally caused less of a deleterious effect on the electrophysiology and network properties of PS19 neurons. One possible explanation for this is that these neurons were already operating under reduced network function, and therefore may be primed to operate under stressful conditions. The inflammatory stimulus may be less able to do so much harm when these networks are already dysfunctional.

It is evident that neuroinflammation simulated by challenging with MgCM causes dysregulation of both neural activity and calcium homeostasis. These findings suggest that neuroinflammation plays a role as an early trigger that initiates the cascade of biological dysfunction that leads to the devastating effects of Alzheimer's. Additionally, our data indicate that the effects of abnormal Tau on the brain manifest far earlier than previous research has proposed, as there is significant neural network dysfunction in the presence of an early pathological form Tau. This suggests that Tau's role in AD pathogenesis may be far earlier than is thought, which is consistent with other literature such as Braak et al.'s proposed staging of Alzheimer's based on Tau accumulation in the brain.<sup>18</sup> If this is true, our findings present a novel opportunity for early treatment and/or prevention of AD. Additional research on this matter should be done to determine whether neurodegenerative disease progression can be slowed or halted by counteracting the effects of neuroinflammation and/or by minimizing early post-translational modifications of Tau in the brain.

### **Acknowledgements:**

I'd like to acknowledge the University of North Carolina at Chapel Hill Department of Neurology, as well as NIH grant R01 NS108808 and NC TraCS ECBR004, for providing the resources for this thesis. This research project would not have been possible without the guidance of Dr. Rick Meeker and Dr. Thomas DeMarse. Dr. Meeker has been an invaluable mentor throughout my three and a half years in his lab and I thank him for creating such an incredible laboratory environment that allowed me to participate in research about which I am very passionate. Dr. DeMarse introduced me to electrophysiology and taught me the necessary skills to operate and collect data from MEAs. Dr. DeMarse also provided data analysis for

electrophysiology that this thesis depended on, so I especially thank him for that. I also thank Dr. Amy Maddox and my thesis group for helping me polish this honors thesis.

## **References:**

1. Heppner, F. L., Ransohoff, R. M. & Becher, B. Immune attack: The role of inflammation in Alzheimer disease. *Nat. Rev. Neurosci.* 16,358–372 (2015).
2. Busche MA, Konnerth A. Impairments of neural circuit function in Alzheimer's disease. *Philos Trans R Soc Lond B Biol Sci.* 2016;371(1700):20150429.
3. Canter, R. G., Penney, J. & Tsai, L. H. The road to restoring neural circuits for the treatment of Alzheimer's disease. *Nature* 539,187–196 (2016).
4. Vossel KA, Ranasinghe KG, Beagle AJ, et al. Incidence and impact of subclinical epileptiform activity in Alzheimer's disease. *Ann Neurol.* 2016;80(6):858-870.
5. Roberson, E. D., Scarce-Levie, K., Palop, J. J., Yan, F., Cheng, I. H., Wu, T., Gerstein, H., Yu, G. Q. and Mucke, L. (2007). Reducing Endogenous Tau Ameliorates Amyloid beta-induced Deficits in an Alzheimer's Disease Mouse Model. *Science* 316, 750-4.
6. Yoshiyama, Y. et al. Synapse Loss and Microglial Activation Precede Tangles in a P301S Tauopathy Mouse Model. *Neuron* 53,337–351 (2007).
7. Bragg, D. C., Boles, J. C. & Meeker, R. B. Destabilization of neuronal calcium homeostasis by factors secreted from choroid plexus macrophage cultures in response to feline immunodeficiency virus. *Neurobiol Dis* 9, 173-186, doi:10.1006/nbdi.2001.0459 (2002).
8. Meeker, R. B., Poulton, W., Clary, G., Schriver, M. & Longo, F. M. Novel p75 neurotrophin receptor ligand stabilizes neuronal calcium, preserves mitochondrial movement and protects against HIV associated neuropathogenesis. *Experimental Neurology* 275 Pt 1, 182-198, doi:10.1016/j.expneurol.2015.09.012 (2016).
9. Meeker, R. B., Poulton, W., Feng, W. H., Hudson, L. & Longo, F. M. Suppression of immunodeficiency virus-associated neural damage by the p75 neurotrophin receptor ligand, LM11A-31, in an in vitro feline model. *J Neuroimmune Pharmacol* 7, 388-400, doi:10.1007/s11481-011-9325-0 (2012).
10. Kuchibhotla, K. V. *et al.* Abeta plaques lead to aberrant regulation of calcium homeostasis in vivo resulting in structural and functional disruption of neuronal networks. *Neuron* 59, 214-225, doi:10.1016/j.neuron.2008.06.008 (2008).
11. Anon (n.d.) B6;C3-Tg(Prnp-MAPT\*P301S)PS19Vle/J. The Jackson Laboratory Available at: <https://www.jax.org/strain/008169> [Accessed March 7, 2019].

12. Alagapan S, Franca E, Pan L, Leondopoulos S, Wheeler BC, DeMarse TB. Structure, Function, and Propagation of Information across Living Two, Four, and Eight Node Degree Topologies. *Front Bioeng Biotechnol.* 2016;4:15. Published 2016 Feb 29. doi:10.3389/fbioe.2016.00015
13. Pan, L. et al. An in vitro method to manipulate the direction and functional strength between neural populations. *Front. Neural Circuits* 9,32 (2015).
14. Potter, S. M. & DeMarse, T. B. A new approach to neural cell culture for long-term studies. *J Neurosci Methods* 110, 17-24 (2001).
15. Tseng JH, Xie L, Song S, et al. The Deacetylase HDAC6 Mediates Endogenous Neuritic Tau Pathology. *Cell Rep.* 2017;20(9):2169-2183.
16. Buzsáki G, Csicsvari J, Dragoi G, Harris K, Henze D, Hirase H (2002) Homeostatic maintenance of neuronal excitability by burst discharges in vivo. *Cereb Cortex* 12:893–899.
17. Bonifazi, P., Goldin, M., Picardo, M.A., Jorquera, I., Cattani, A., Bianconi, G., Represa, A., Ben-Ari, Y., and Cossard, R. (2009). GABAergic Hub Neurons Orchestrate Synchrony in Developing Hippocampal Networks. *Science* 326, 1419-1424
18. Braak H, Alafuzoff I, Arzberger T, Kretschmar H, Del Tredici K. Staging of Alzheimer disease-associated neurofibrillary pathology using paraffin sections and immunocytochemistry. *Acta Neuropathol.* 2006;112(4):389-404.